

Kondo-semimetal to Fermi-liquid phase crossover in black phosphorus to pressure-induced orbital-nematic gray phosphorus

L. Craco,^{1,2} T. A. da Silva Pereira,¹ S. R. Ferreira,¹ S. S. Carara,¹ and S. Leoni³

¹*Instituto de Física, Universidade Federal de Mato Grosso, 78060-900, Cuiabá, MT, Brazil*

²*IFW Dresden, Institute for Solid State Research, P.O. Box 270116, D-01171 Dresden, Germany*

³*School of Chemistry, Cardiff University, Cardiff, CF10 3AT, United Kingdom*



(Received 7 March 2018; revised manuscript received 28 June 2018; published 12 July 2018)

We perform a comparative study of the electronic structures and electrical resistivity properties of black (A17) and of pressurized gray (A7) phosphorus, showing band-selective Kondo-like electronic reconstruction in these layered *p*-band phosphorus allotropes. Based on density functional dynamical mean-field theory calculations, we show that gray phosphorus can host a three-dimensional Kondo semimetal to a Fermi liquid phase crossover under anisotropic compression, which lifts in-layer orbital degeneracy. Therein, the *3p* spectrum is almost unaffected both in the semiconducting and semimetallic Kondo phases, however in the Fermi liquid regime strong electronic reconstruction is predicted to exist in the orbital nematic phase of compressed gray phosphorus. These findings contribute to the microscopic understanding of the role played by dynamical multiorbital electronic interactions in the low energy spectrum of correlated semiconductors and topological semimetals.

DOI: [10.1103/PhysRevB.98.035114](https://doi.org/10.1103/PhysRevB.98.035114)

I. INTRODUCTION

Black phosphorus (BP, not to be misunderstood as boron phosphide) is the thermodynamic most stable allotrope of elemental phosphorus at normal conditions [1]. In its A17 orthorhombic crystal structure layers of six-membered rings with chair conformation are stacked along [010]. Alternatively, a single layer can be decomposed into sets of interconnected zigzag chains on two different planes. Therein, phosphorus atoms are threefold connected. The layers are held together by van der Waals forces into a three-dimensional crystal as shown in the left panel of Fig. 1. Despite its classic status as an element [2], phosphorus remains surprising due to fascinating structure/property relationships hosted by this layered *p*-band material [3]. Particularly interesting are strain-induced band gap modifications [4–6], which allows us to tune semiconductor BP into anisotropic Dirac semimetal [7], and a superconducting phase transition induced by pressure [8]. In the latter, selective low-energy electronic reconstruction suggests placing BP among correlated electron systems, like pointed out elsewhere [9].

The one-particle band gap of multilayer and bulk BP [10] as well as in BP films [11] remains an open problem of current interest. *Ab initio* density functional calculations of bulk BP yield a band gap in the range of 0.3 eV to 0.35 eV [12], a value compatible with scanning tunneling data [13]. However, this gap size appears to be in conflict with transport data by at least two groups [14,15], where the *dc* resistivity measurements at ambient pressures show a temperature-dependence behavior characteristic of narrow band semiconductors with very low activation energies. Band gap estimations for few-layer and bulk BP as well as different GW implementations BP show broad band gap variations in this *p*-band system [10].

Under moderate compression (≈ 5 GPa) BP transforms into the semimetallic rhombohedral α -As type structure (A7), as

displayed in Fig. 1, right panel. While not group-subgroup related, A17 and A7 can be accommodated in a common monoclinic subgroup (*P2/c*) with phosphorus atoms on general Wyckoff positions [16]. Due to its peculiar electronic structure [17], narrow band gap [12] BP displays anisotropic particle-hole excitations [18], magnetoresistance [14,19], and thermal transport properties [20]. Under hydrostatic compression [15,21], electrical resistivity measurements reveal that the one-particle energy gap of orthorhombic BP can be continuously reduced down to zero, which is reached at a critical pressure $P_c \approx 1.25$ GPa [15]. The characteristic low-temperature resistive divergence of semiconducting systems is gradually suppressed. Beyond P_c the resistivity shows semimetallic behavior, which indicates a pressure-induced insulator to semimetal transition [15,22]. Under pressure, two consecutive reversible structural transitions occur: from orthorhombic BP to a rhombohedral phase (gray phosphorus) occurring at 5.5 GPa [23], followed by transformation into a simple-cubic phase at pressures about 11 GPa [24]. Near the semiconductor-to-semimetal transition, applied pressure pushes the valence and the conduction bands together [15], causing substantial changes in the topology of the Fermi surfaces [22]. Hall resistivity measurements of bulk BP close to P_c show in fact evidence of Lifshitz transition.

Sizable electronic reconstruction qualifies therefore pressurized phosphorus as an orbital-selective *p*-band system, hosting renormalized electronic states at low energies. Here, we extend our earlier density functional dynamical mean-field theory study of bulk BP [9] to predict the appearance of intrinsic many-body correlation effects in the electronic structure of A7 gray phosphorus (GP), the high pressure layered polymorph of BP. Careful comparison of the multiorbital (MO) spectral functions of black and gray phosphorus provides insights into the MO correlated electronic behavior of GP. Additionally, we explore the role played by an orbital nematic state, which could be induced via anisotropic compression,

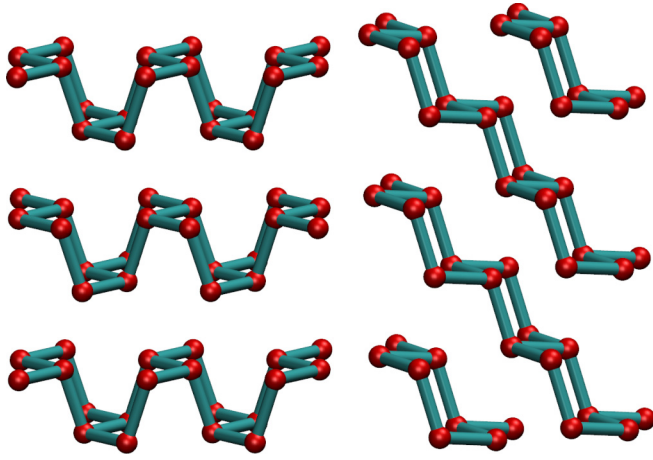


FIG. 1. Layered structure of black (left panel) and gray (right panel) phosphorus. See Ref. [16] for details on the A17 (black) to A7 (gray) structural transformation of pressurized phosphorus.

showing the emergence of a Fermi liquid electronic state at low temperatures.

MO physics is inherently complex due to lattice, charge, and spin degrees of freedom [25]. These coupled correlations have hampered theoretical studies to treat them in a fully realistic way. Density functional plus dynamical mean-field theory (DFT + DMFT) [26] allows for a systematic approach to MO electronic correlation. In MO systems, external perturbations like pressure, lattice distortions, and chemical doping can cause spectacular electronic effects. As an illustration thereof, here we study correlation- and nematic-induced electronic reconstructions using the DFT + DMFT method, which self-consistently takes into account these effects in real materials.

Since electronic correlation is ubiquitous, an interesting question in the context of correlated semiconductors [27,28] is whether many-body correlation effects, characteristic of narrow band materials [25], can also be hosted in p -band semimetals. Based on a realistic model, in this paper we provide a comparative many-particle description of the correlated electronic structure of black and high-pressure gray phosphorus and of its impact on electrical transport. Our results, which are derived from reconstructed spectral functions, reveal that bulk GP hosts a MO Kondo state [29,30], which undergoes to a metallic Fermi liquid state upon lifting the in-plane orbital degeneracy in the high-pressure phase.

The Kondo effect is known as one of the most interesting phenomena in conventional metals [31]. Historically, the Kondo effect occurs in the presence of dilute concentration of localized spins coupled to the Fermi sea of metals [32]. The many-body interaction between the localized spin and conduction electron screens the impurity spin leading to a weak divergent resistance, as one approaches zero temperature. It also results in sharp Kondo resonances in the electron spectral functions of narrow band, Fermi liquid metals [33]. Here, we are particularly interested in emergent Kondo physics in p -band semimetals [34–37], which is expected to be distinct from impurity-induced Kondo effect in conventional metals due to the specific electronic structure of the gapped, semimetallic electron gas at low energies. To date, there are only few theoretical studies and experimental evidences for Kondo-like

physics in graphene [34,35,38], graphite [37], and elemental bismuth [36]. The reason is that the Kondo effect is not easily accessible by experiments on p -band systems. In V -shaped, Dirac-fermion p band materials like graphene and graphite, the low-electron density of states (DOS) near the Dirac point prevents the appearance of correlation-induced Kondo and Fermi liquid fingerprints. The Kondo temperatures, for example, are expected to be extremely small [39]. Therefore, this many-particle effect may be shifted to temperatures, which would be experimentally inaccessible. In transport experiments the Kondo effect is usually manifested by the logarithmic increase of the electrical resistivity at low temperatures [35,40]. The low temperature upturn in resistivity is seen in a variety of systems [41] and can originate from many-particle corrections to resistivity due to weak electron localization, canonical Kondo effect (or the scattering of conduction electrons by localized impurities) or as discussed in the context of carbon nanotubes [30], the Kondo effect in p -band materials can also occur in the absence of spin impurity if orbital degeneracy is present in the system. In such a case, the role of spin is replaced by other degrees of freedom, such as an orbital quantum number, and the leading logarithmic corrections in the electrical resistivity are thus due to the local interactions between electrons on different orbitals [29].

Although Kondo-like physics has been studied in the context of p -band materials [34–38], there has been no theoretical attempt to describe the emergence of orbital Kondo effect [29,30] and its crossover to a Fermi regime in phosphorus allotropes. In this paper we present a comprehensive DFT + DMFT analysis for the correlated MO problem of A7 GP to show that an emergent orbital Kondo effect in a p -band system can be tuned towards a Fermi liquid state via distortion induced orbital-nematic order with lifting twofold orbital degeneracy. Within local density approximation plus dynamical mean-field theory (LDA + DMFT) [26] framework we show that the concomitant interplay between MO electronic interactions and twofold orbital degeneracy in the $p_{x,y}$ orbitals of GP gives rise to an orbital Kondo effect, implying the formation of orbital singlets at low temperatures as in carbon nanotubes [30]. Additionally we show that the twofold orbital degeneracy of A7 phosphorus can be lifted by an orbital field which can be tuned via uniaxial compression in the bulk. We demonstrate the presence of distinct low-energy frequency dependence behavior of the electronic self-energies and their relation to electrical transport across the orbital Kondo to Fermi liquid phase crossover.

II. RESULTS AND DISCUSSION

BP (space group $Cmca$) is a narrow band gap semiconductor under ambient pressure conditions [15]. Its orthorhombic crystal structure consists of corrugated layers of six-membered rings stacked along the [010] direction (see Fig. 1, left panel). As in the case of bulk BP, the individual layers of A7 phosphorus are also connected by van der Waals forces. GP has a rhombohedral structure (space group $R3m$) [24], similar to elemental bismuth [36]. Being a homologue of Bi and As, A7 phosphorus is characterized by extended puckered layers of three-connected phosphorus atoms, with shorter distances within each layer than between (111) layers. Upon

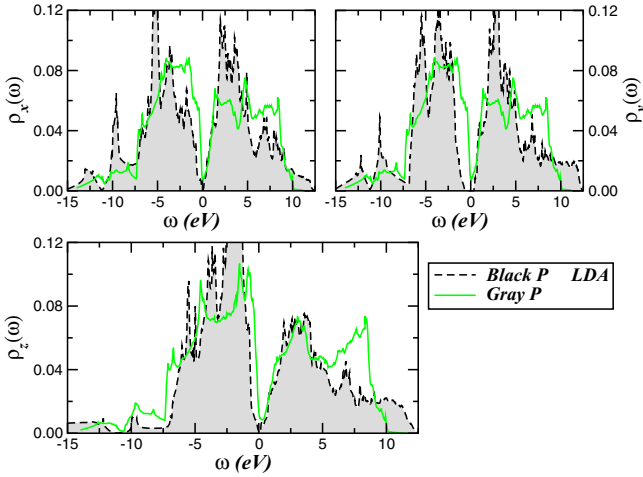


FIG. 2. Comparison between the LDA orbital resolved density of states (DOS) for bulk BP (dashed line) and GP (solid line), showing sizable one-particle band narrowing of the conduction band states of bulk GP. Notice as well the (narrow gap) insulating and semimetallic nature of BP and GP, respectively.

rhombohedral distortion, semiconducting A17 phosphorus becomes a p -band semimetal with a small number of valence band states at the Fermi energy (E_F), as shown in Fig. 2. Here, LDA calculations for the crystal structure at real conditions were performed using the linear muffin-tin orbitals (LMTO) [42,43] scheme in the atomic sphere approximation. More precisely, calculations were performed using the scalar relativistic version of the PY-LMTO [43]. Similar to BP [9], the total density was converged on a grid of 301 irreducible k points, and the radii of the atomic spheres were chosen as $r = 2.74$ a.u. in order to minimize their overlap. The corresponding orbital resolved LDA DOS is shown in Fig. 2. As seen, BP shows a marked anisotropy near E_F , which reflects structural differences within the layers (x, y directions) and along the stacking (z direction). This anisotropy is of top importance in understanding transport properties consistent with a narrow gap scenario, like demonstrated elsewhere [9].

In contrast with BP, the orbital resolved spectral functions of GP show an appreciable one-particle band narrowing (≈ 2.15 eV) of the conduction band states at high energies and a suppression of the one-electron band gap centered near E_F . Similar to bismuth [36], elemental phosphorus has a formal +3 oxidation state, which implies half occupation in the p sector. Upon A17 to A7 phase transformation all electronic $3p$ carriers acquire some itinerance, which provides valence and conduction band states in all active $3p$ -(x, y, z) orbitals near E_F . This situation of three half-filled semimetallic bands and twofold (x, y) orbital degeneracy provides the underlying microscopic one-band seeds of an orbital Kondo scenario [30] in A7 phosphorus.

A. Role of multiorbital electronic correlations

The many-body MO Hamiltonian relevant for bulk phosphorus is $H = H_0 + H_{\text{int}}$ [9] with

$$H_0 = \sum_{\mathbf{k}a\sigma} \epsilon_a(\mathbf{k}) c_{\mathbf{k}a\sigma}^\dagger c_{\mathbf{k}a\sigma}, \quad (1)$$

and

$$H_{\text{int}} = U \sum_{ia} n_{ia\uparrow} n_{ia\downarrow} + \sum_{ia \neq b} U' n_{ia} n_{ib} - J_H \sum_{ia \neq b} \mathbf{S}_{ia} \cdot \mathbf{S}_{ib}. \quad (2)$$

Here, $a = x, y, z$ label the diagonalized $3p$ bands and $\epsilon_a(\mathbf{k})$ is the one-electron band dispersion, which encodes details of the one-electron (LDA) band structure. To label the x, y, z orbitals of GP we have used the same reference system as in the work by Y. Hayasi *et al.* [17] and in Ref. [9]. $U' \equiv U - 2J_H$, with U, U' being the intra- and interorbital Coulomb repulsion and J_H is Hund's rule coupling. Within LDA the one-band dispersions are read off from $\epsilon_a(\mathbf{k})$: These are inputs for MO LDA + DMFT which generates, respectively, Kondo insulating and semimetallic states in bulk A17 and A7 phosphorus as discussed below.

We use MO DMFT for the three-orbital model of bulk phosphorus with the MO iterated-perturbation theory (MO-IPT) as an impurity solver of the many-particle problem in DMFT [44–46]. This method has been benchmarked by comparison with numerically exact continuous time quantum Monte Carlo method (CTQMC) as an impurity solver in DMFT [46], where very good accord between IPT and CTQMC for both one-band and multiband Hubbard models was found. The MO LDA + DMFT scheme [26] adequately describes the effect of local dynamical interactions in the limit of large lattice dimensions (DMFT) [33]. Thereby, practical calculations become feasible even for broad p -band systems [9,36]. The basic idea in a DMFT solution involves replacing the lattice model by a self-consistently embedded MO-Anderson impurity model, and the self-consistency condition requiring the local impurity Green's function to be equal to the local Green's function for the lattice. The full set of equations for the MO case can be found in Refs. [44–46], so we do not repeat the equations here. It is worth mentioning, however, that the IPT is an interpolative *ansatz* that connects the two exactly soluble limits of the one-band Hubbard model [47], namely, the uncorrelated ($U = 0$) and the atomic ($\epsilon_{\mathbf{k}} = 0$) limits. At intermediate U , it ensures the correct low- and high-energy behavior of the self-energies and spectral functions. Finally, it ensures the Mott-Hubbard metal-insulator transition from a correlated metal to a Mott insulator that occurs as a function of the Coulomb interaction U [25].

Since the effect of electronic interactions in the excitation spectrum of phosphorus allotropes is quite subtle and not fully understood, in Fig. 3 we compare the LDA and LDA + DMFT orbital-resolved spectral functions that emerges from dynamical MO interactions in bulk GP. As in our earlier study of bulk BP [9], LDA + DMFT results for $U = 10$ eV and $J_H = 0.5$ eV are shown in Fig. 3. Our choice for U is consistent [9] with a Hartree-Fock estimation of intra-atomic Coulomb energy [48] and places bulk BP on the Kondo insulating side of the correlated semiconducting family [27]. Figure 3 shows the emergence of a narrower (compared to LDA) semimetallic band gap at low energies in the electronic spectrum of GP with concomitant appearance of incipient lower- and upper-Hubbard bands on different orbitals at high energies. Even if the U/W parameter ratio used here is small (W is the one-particle LDA bandwidth), MO dynamical correlations arising from

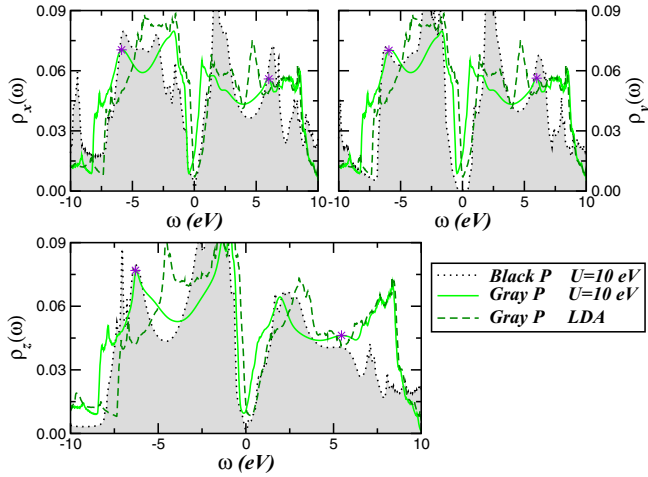


FIG. 3. LDA (dashed line) and LDA + DMFT (solid line) orbital resolved DOS of bulk GP, showing spectral weight redistribution over large energy scales. The LDA + DMFT spectral functions of BP are shown for comparison. The stars indicate the energy position of the incipient lower- and upper-Hubbard bands in the valence and conduction band states of bulk BP.

U, U' lead to spectral weight redistribution over large energy scales. While the spectral lineshape close to E_F remains close to that found in LDA for BP [9], large transfer of spectral weight is obtained in GP compared to BP due to its reduced one-particle bandwidth and, thus, enhanced many-body correlation effects. As in the case of bulk BP [17], future polarized soft-x-ray emission and absorption spectroscopy are called for to confirm our prediction for the reconstructed electronic spectrum of pressurized GP.

As a further illustration of the correlated nature of our spectral functions near the gap (BP) or pseudogap (GP) energy scale, in Fig. 4 we show the changes in the orbital-resolved imaginary parts of the self-energies $[Im\Sigma_a(\omega)]$. Remarkably, $Im\Sigma_a(\omega)$ vanishes in the region of the semiconducting and

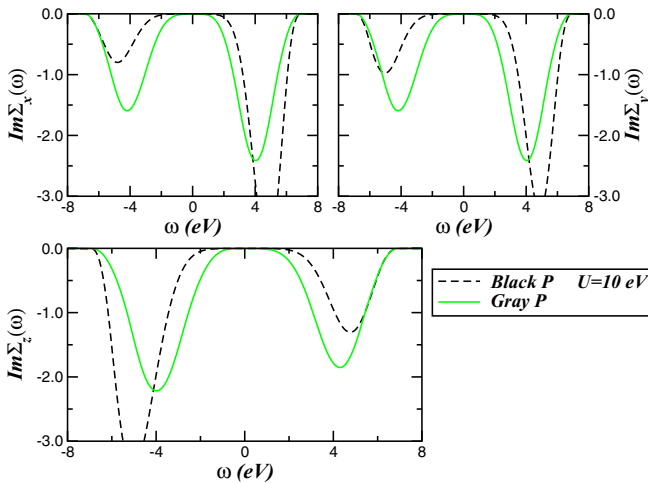


FIG. 4. Imaginary part of the orbital-resolved self-energies $[Im\Sigma_a(\omega)]$ within the Kondo insulating phases of bulk BP and GP. Notice the substantial reduction of the near zero constant value of $[Im\Sigma_a(\omega)]$ near E_F in GP, implying stronger Kondo correlations effects in GP compared to BP.

semimetallic band gaps of BP and GP, as it occurs with the correlated self-energies of periodic Anderson lattice models [45,49], which are known to capture intrinsic Kondo-like physics within the DMFT approximation. This interesting low-energy scale aspect is characteristic of Kondo insulators, in which the gap arises due to sizable interband hybridization between the localized and the conduction electrons [45,49]. Sizable correlation effects manifest themselves above the gap (BP) and pseudogap (GP) scales as negative bump structures, as is apparent from the orbital-resolved self-energies. This unveils an underlying Kondo-like physics as in graphite [37]. Stronger electronic correlations imply a reduction of the vanishing region in the GP MO self-energies (Fig. 4). Proximity to an anisotropic Kondo semimetallic state is indicated by the narrowing of the negative bump structures lying above and below the Fermi energy, $E_F (= \omega = 0)$. Spectral redistribution in response to additional small perturbations (like external anisotropic compression) can drive it into a true metallic state, which hosts quadratic ω dependence in $Im\Sigma_a(\omega)$ at low temperatures, as shown below. This is a manifestation of the intrinsically correlated nature of the system of interest.

Additionally, to elucidate close similarities between the semiconducting and semimetallic states found for BP and GP at $U = 10$ eV as well as the crucial role played by MO interactions on electrical transport in layered phosphorus-based p -band materials the temperature (T) dependence of the dc resistivity is computed using the orbital resolved LDA + DMFT spectral functions. Within the Kubo formalism [50], the dc conductivity can be expressed as

$$\sigma_{dc}(T) = \frac{2\pi e^2}{\hbar V} v^2 \sum_a \int d\epsilon \rho_a^{(0)}(\epsilon) \int d\omega A_a^2(\epsilon, \omega) [-f'(\omega)], \quad (3)$$

where $\rho_a^{(0)}(\epsilon)$ is the LDA DOS,

$$A_a(\epsilon, \omega) = -\frac{1}{\pi} Im \frac{1}{\omega + \mu - \Sigma_a(\omega) - \epsilon} \quad (4)$$

is the LDA + DMFT spectral function, $a = (x, y, z)$ represents the three $3p$ orbitals, μ is the chemical potential, v is the average carrier velocity, $f(\omega)$ is the Fermi function, and V the sample volume. Based on this formalism, in Fig. 5 we display the T dependence of electrical resistivity $[\rho_{dc}(T) \equiv 1/\sigma_{dc}(T)]$ computed using the LDA + DMFT orbital resolved spectral functions, Eq. (4), for $U = 10$ eV in Eq. (3) above. Interestingly, $\rho_{dc}(T \rightarrow 0)$ of BP is very large with clear semiconductinglike behavior at low temperatures, in accordance with the insulating scenario shown in Fig. 3. Similar T dependence as in Fig. 5 has been observed [14], indicating that the exponential increase of $\rho_{dc}(T)$ at low T is governed by an intrinsically small band gap. Equally consistently with experimental observations [14], as temperature is decreased from high T (≈ 250 K in experiment), ρ_{dc} decreases in a metallic form reaching a minimum value around 40 K.

The agreement between theory and experiment is rather good, despite a somehow higher experimental value close to 60 K. This gives us confidence to further explore the electrical transport behavior of semimetallic A7 phosphorus. Figure 5 displays our LDA + DMFT results for the electrical resistivity of bulk GP. Due to its intrinsic semimetallic nature, the strongly localized behavior of BP is partially suppressed

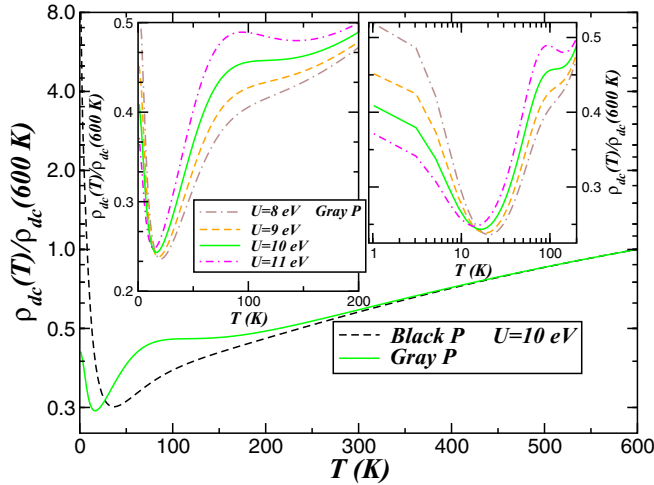


FIG. 5. T dependence of electrical resistivities for the Kondo insulating state and semimetallic states of bulk BP and GP, respectively, showing qualitative good accord with transport data [14,15] for bulk BP. Particularly interesting is the insulating behavior at low temperatures intrinsic to narrow band semiconductors and the minimum value around 40 K in BP, which is pushed to lower temperatures in semimetallic GP. Noteworthy is the region, where $\rho(T)$ is linear in $\ln(T)$ for bulk GP (as seen in the right inset), the fingerprint of Kondo resistivity. Left inset displays the resistivity curves of GP for different U values, showing the changes in the $\ln(T)$ corrections at low temperatures due to increased metallicity in the bulk.

in pressurized A7 phosphorus with concomitant reduction of the Kondo temperature ($T_K \approx 16$ K for GP with $U = 10$ eV), or the temperature below which $\rho_{dc}(T)$ display an insulating upturn. Particularly interesting is the Kondo resistivity (see the right inset of Fig. 5) in the region where $\rho_{dc}(T)$ is linear in $\ln(T)$ [35,40], which according to our description arises from the interplay between x,y -orbital degeneracy [30] and U' -induced MO Kondo effect within DMFT [29]. Moreover, in the right inset of Fig. 5 we display the changes in the $\ln(T)$ corrections for different values of the on-site Coulomb repulsion U . Interestingly, the T dependence in the left inset of Fig. 5 resembles the one seen in experiments of pressurized phosphorus, [15] showing significant changes in the low- T resistivity upturn. This might be the precursor for the pressure-induced insulator-metal transition in elemental phosphorus. Based on our results in Fig. 4 it can plausibly be assumed that noticeable electronic reconstruction occurs in pressurized GP at low pressures. Taken together, these results support a description of bulk GP as correlated semimetal, proximate to a low- T Fermi liquid metal as shown below.

B. Role of lifting twofold orbital degeneracy

Under external perturbations like pressure or lattice strain, the hopping elements and the crystal field splittings are renormalized in nontrivial ways. In practice however, it is very difficult to separate the effects of the hopping from those induced by crystal field splittings, even more so if lattice instabilities under pressure or negative pressure are not known a priori. Accordingly, since a semimetal-to-metal

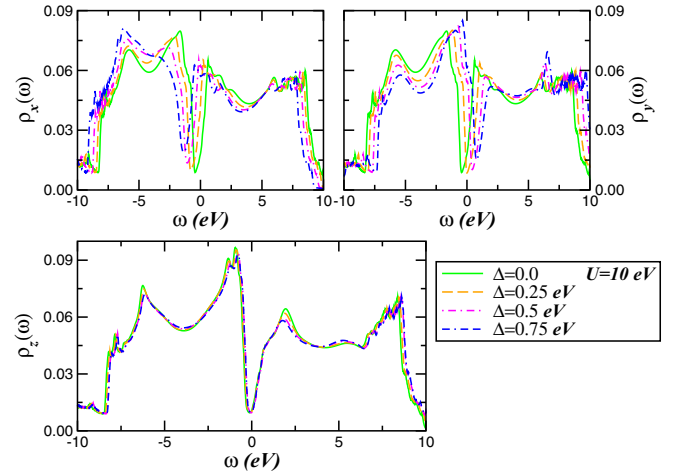


FIG. 6. Orbital resolved LDA + DMFT ($U = 10.0$ eV, $J_H = 0.5$ eV) spectral functions in the orbital nematic phase of bulk GP, showing their evolution with increasing the orbital field Δ . The anisotropic energy gap suppression in the valence and conduction bands of the p_x and p_y orbitals on increasing Δ goes hand-in-hand with large scale spectral weight transfer. Particularly interesting are the crossing points at different energies in the spectral functions.

crossover which is likely to exist in the metastable phases [3] of phosphorus at low pressures, we adopt the following strategy to derive this crossover. Instead of actually lifting orbital degeneracy by uniaxial compression, we search for an instability of the semimetal phase to the paramagnetic Fermi liquid metal. Here, we follow the methodology used in earlier studies addressing the effect of orbital splittings on the correlated many-body states of transition metal oxides [51] and more recently to pressurized FeS [52] and solid oxygen [53]. We consider the orbital-dependent on-site energy term,

$$H_\Delta = \sum_{i\alpha\sigma} \Delta_\alpha n_{i\alpha\sigma}, \quad (5)$$

in the p -band MO Hamiltonian of GP, i.e., $\tilde{H} = H_0 + H_{\text{int}} + H_\Delta$. In our self-consistent MO treatment we vary the trial Δ in small steps, keeping $\Delta_x = \Delta$, $\Delta_y = -\Delta$, to simulate the structural (and hence, electronic) changes upon uniaxial compression. This choice in H_Δ directly leads to $\langle n_y \rangle > \langle n_x \rangle$ by itself, implying a ferro-orbital order along with a finite orbital nematicity,

$$\langle N \rangle \equiv \frac{\langle n_y \rangle - \langle n_x \rangle}{\langle n_x \rangle + \langle n_y \rangle} \neq 0, \quad (6)$$

as discussed in the context of iron arsenide superconductors [54]. In our theory, Δ_a acts like an external field in the orbital sector (orbital fields), sensitively controlling the occupations of each orbital in much the same way as the magnetization of a paramagnet as function of an external magnetic, Zeeman field.

Figure 6 shows that small variations of Δ with fixed U and J_H drive appreciable spectral weight transfer, producing orbital polarization and selective electronic reconstruction of the one-particle spectral functions. While the correlated DOS of the p_z orbital remains similar to the undistorted A7 phosphorus, p_x and p_y are clearly affected by the orbital field Δ , showing large transfer of spectral weight with increasing Δ . As seen the

p_z DOS remains semimetallic, while the $p_{x,y}$ bands undergo a semimetal-to-metal phase crossover with emergence of coherent Kondo peaks at E_F . The underlying theoretical reason for this is as follows: With increasing Δ scattering between the effectively semilocalized (p_z) and itinerant components ($p_{x,y}$) of the matrix DMFT propagators produces a Fermi liquid metal because of strong interband scattering operates in an orbitally polarized metallic system. Our results thus suggest that in broad band systems small changes in crystal field splittings might promote local orbital fluctuations which cuts off the Kondo scattering of the semimetallic channels. From our results, the orbital-selective Kondo semimetallic phase is thereby suppressed in distorted GP with broken twofold rotation symmetry, leading to continuous evolution of the coherent, semimetal to a correlated Fermi liquid like metal as shown below.

Expanding on our previous discussion, in what follows we provide a microscopic interpretation for the semimetallic-to-metallic crossover in GP and its implication to anisotropic electronic mobilities in the nematic state in depth. Specifically, in addition to the orbital-selective electronic reconstruction revealed in Fig. 6, we show that the imaginary parts of the electronic self-energies are reshaped as well and correlate with the evolution of the LDA + DMFT spectral functions with Δ . This in our opinion reinforces the basic hypothesis about the interplay between structural distortions (inducing changes in crystal field splittings) and sizable MO many-body correlations in bulk p band systems [53]. Given the large dynamical spectral weight transfer characteristic of correlated electron systems, orbital nematicity (or the lifting of the twofold orbital degeneracy within the x,y orbitals of GP) can be expected to have a sensible impact on correlated semiconductors and semimetals in close proximity to electronic [15] and metastable structural phase transformations [3]. The generic appearance of metallic states and the instabilities of such states to, for example, unconventional superconductivity [3] makes this a very important question worth investigating, which may open scenarios on pressurized BP.

In Fig. 7 gradual changes in the self-energy imaginary parts of GP from the orbital-Kondo to a MO Fermi liquid regime with increasing Δ are shown. Intriguingly, orbital-Kondo to orbital-selective Fermi-liquid crossover occurs simultaneously in all orbitals. Albeit not directly reflected in a pronounced electronic reconstruction of the one-particle p_z -DOS as shown in Fig. 6, the frequency dependence of $Im\Sigma_z(\omega)$ does show $-\omega^2$ Fermi liquid dependence as Δ increases toward to larger values. This in turn suggests that in broad band electron systems correlation effects might not be directly probed by spectroscopy experiments but they might be hidden in the correlated self-energies as recently shown for bulk BP [9]. Also interesting in Fig. 7 is the clear Fermi liquid energy dependence of $Im\Sigma_y(\omega)$, implying that this is the most correlated $3p$ orbital sector due to enhanced electronic states near E_F in the distorted bulk. This prediction could be corroborated by future spectroscopy and transport experiments probing anisotropic (in-plane and out-of-plane) spectral functions and electronic mobilities in the orbital nematic state of bulk GP.

To gain insights on the interplay between electron-electron interactions and orbital nematicity on the multiple structure of the GP, in Fig. 8 we display the temperature dependence

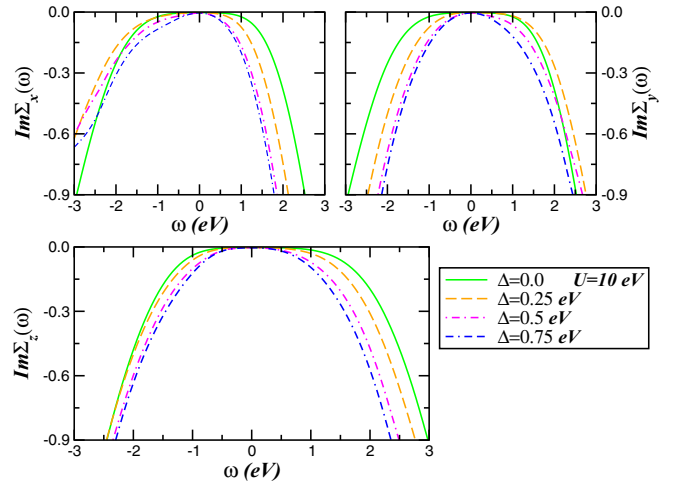


FIG. 7. Orbital-resolved self-energies (imaginary part, $[Im\Sigma_a(\omega)]$) across the Kondo insulating to Fermi liquid crossover of orbital nematic GP. Notice the substantial reduction of the near zero constant value of $[Im\Sigma_a(\omega)]$ near E_F in all channels upon increasing the orbital field Δ and the smooth crossover to a $-\omega^2$ dependence characteristic of correlated Fermi liquid metals.

of the electrical resistivity showing its evolution from a Kondo semimetal to a metallic Fermi liquid behavior on increasing the orbital field Δ . As visible in the inset of Fig. 8 at $\Delta = 0.75$ eV the temperature dependence of resistivity follows Fermi liquid behavior with a quadratic dependence at low temperatures. Meanwhile, the $\ln(T)$ dependence observed in Kondo systems is still found at Δ values below 0.3 eV. Interesting as well is the fact that for $0.35 < \Delta < 0.5$ eV we obtain an almost linear T dependence, usually referred to as non-Fermi liquid behavior. Even though the nature of non-Fermi liquid state is in debate and the variation from the T to T^2 dependence

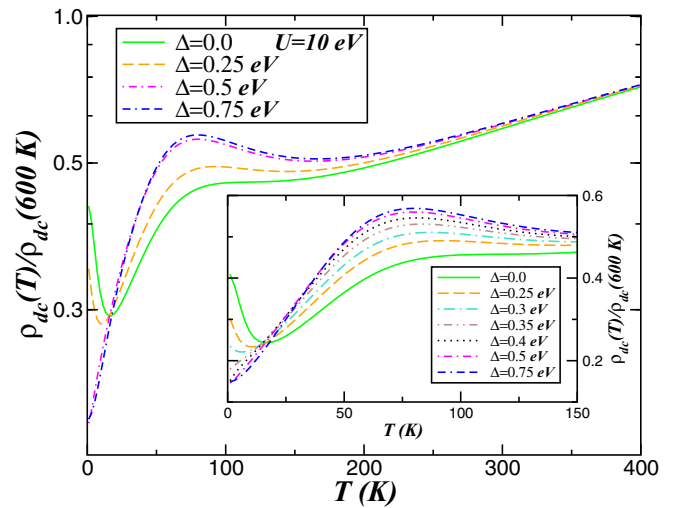


FIG. 8. T dependence of electrical resistivities for the Kondo semimetallic and metallic state of orbital nematic GP. Particularly interesting is the suppression of the $\ln(T)$ behavior and the resistivity upturn with increasing Δ . The inset displays resistivity curves of GP for the different Δ values on a linear scale, showing the changes in $\rho(T)$ towards a T^2 dependence characteristic of Fermi liquid metals.

with doping, pressure, and “chemical pressure” are considered as common characteristics in the cuprates and iron-based superconductors, to the best of our knowledge it has never been considered in the context of Kondo to Fermi liquid crossover of broad band p band systems. Taken together, our results in Figs. 7 and 8 indicate that enhancement of electronic correlations upon uniaxial compression could promote higher- T_c superconductivity hitherto not probed yet in pressurized phosphorus allotropes and related p band systems.

III. CONCLUSION

In this work we have studied the role of multiorbital electronic correlations in bulk BP and GP allotropes, showing the existence of semimetallic Kondo-like behavior in the electronic and transport properties of bulk GP. We have also explored the interplay between sizable electronic correlations and in-plane rotational symmetry breaking in bulk GP and the emergence of an orbital nematic phase, which is likely to exist in compressed GP. The unusual anisotropic character of electronic and charge transport induced by an orbital nematic state with lifted twofold orbital degeneracy reveals an orbital-selective Kondo to Fermi liquid phase crossover. This arises from low-energy scatterings having their origin in the competition between pressure

induced semimetallicity and orbital nematicity within the LDA + DMFT approximation. Taken together, many-particle electron-electron correlation effects are predicted to be important for the occurrence of emergent orbital Kondo and Fermi liquid behavior in topological Dirac and Weyl semimetals [55] without embedded impurities [56].

ACKNOWLEDGMENTS

L.C.’s work is presently supported by CNPq (Grant No. 304035/2017-3). L.C. thanks M. A. Gusmão for useful comments and discussions. S.L. acknowledges support from the UK Research Council for using work in the paper that was undertaken by a student under Project No. EP/M50631X/1 as well as the DFG for support under the priority project SPP1415 and for a personal Heisenberg grant. S.L. also thanks ZIH Dresden and ARCCA Cardiff for computational resources. Via S.L.’s membership of the UK’s HPC Materials Chemistry Consortium, which is funded by EPSRC (No. EP/L000202), this work made use of the facilities of ARCHER, the UK’s National High-Performance Computing Service, which is funded by the Office of Science and Technology through EPSRC’s High End Computing Programme. S.L. wishes to thank Min Gao for insightful discussions.

-
- [1] A. Morita, *Appl. Phys. A* **39**, 227 (1986); H. Liu, Y. Du, Y. Deng, and P. D. Ye, *Chem. Soc. Rev.* **44**, 2732 (2015).
 - [2] P. W. Bridgman, *J. Am. Chem. Soc.* **36**, 1344 (1914).
 - [3] J. A. Flores-Livas, A. Sanna, A. P. Drozdov, L. Boeri, G. Profeta, M. Eremets, and S. Goedecker, *Phys. Rev. Materials* **1**, 024802 (2017).
 - [4] R. Fei, V. Tran, and L. Yang, *Phys. Rev. B* **91**, 195319 (2015).
 - [5] A. S. Rodin, A. Carvalho, and A. H. Castro Neto, *Phys. Rev. Lett.* **112**, 176801 (2014).
 - [6] G. Qin, Q.-B. Yan, Z. Qin, S.-Y. Yue, H.-J. Cui, Q.-R. Zheng, and G. Su, *Sci. Rep.* **4**, 6946 (2014).
 - [7] J. Kim, S. S. Baik, S. H. Ryu, Y. Sohn, S. Park, B.-G. Park, J. Denlinger, Y. Yi, H. J. Choi, and K. S. Kim, *Science* **349**, 723 (2015).
 - [8] I. Shirovani, J. Mikami, T. Adachi, Y. Katayama, K. Tsuji, H. Kawamura, O. Shimomura, and T. Nakajima, *Phys. Rev. B* **50**, 16274 (1994).
 - [9] L. Craco, T. A. da Silva Pereira, and S. Leoni, *Phys. Rev. B* **96**, 075118 (2017).
 - [10] A. N. Rudenko, Shengjun Yuan, and M. I. Katsnelson, *Phys. Rev. B* **92**, 085419 (2015).
 - [11] B. Deng, V. Tran, Y. Xie, H. Jiang, C. Li, Q. Guo, X. Wang, H. Tian, S. J. Koester, H. Wang, J. J. Cha, Q. Xia, L. Yang, and F. Xia, *Nat. Commun.* **8**, 14474 (2017).
 - [12] Z. S. Popović, J. M. Kurdestany, and S. Satpathy, *Phys. Rev. B* **92**, 035135 (2015).
 - [13] B. Kiraly, N. Hauptmann, A. N. Rudenko, M. I. Katsnelson, and A. A. Khajetoorians, *Nano Lett.* **17**, 3607 (2017).
 - [14] Z. Hou, B. Yang, Y. Wang, B. Ding, X. Zhang, Y. Yao, E. Liu, X. Xi, G. Wu, Z. Zeng, Z. Liu, and W. Wang, *Sci. Rep.* **6**, 23807 (2016).
 - [15] Z. J. Xiang, G. J. Ye, C. Shang, B. Lei, N. Z. Wang, K. S. Yang, D. Y. Liu, F. B. Meng, X. G. Luo, L. J. Zou, Z. Sun, Y. Zhang, and X. H. Chen, *Phys. Rev. Lett.* **115**, 186403 (2015).
 - [16] S. E. Boulfelfel, G. Seifert, Y. Grin, and S. Leoni, *Phys. Rev. B* **85**, 014110 (2012).
 - [17] Y. Hayasi, T. Takahashi, H. Asahina, T. Sagawa, A. Morita, and I. Shirovani, *Phys. Rev. B* **30**, 1891 (1984).
 - [18] R. Schuster, J. Trinckauf, C. Habenicht, M. Knupfer, and B. Büchner, *Phys. Rev. Lett.* **115**, 026404 (2015).
 - [19] S. Hu, J. Xiang, M. Lv, J. Zhang, H. Zhao, C. Li, G. Chen, W. Wang, and P. Sun, *Phys. Rev. B* **97**, 045209 (2018).
 - [20] Y. Wang, G. Xu, Z. Hou, B. Yang, X. Zhang, E. Liu, X. Xi, Z. Liu, Z. Zeng, W. Wang, and G. Wu, *Appl. Phys. Lett.* **108**, 092102 (2016).
 - [21] Y. Akahama, S. Endo, and S. Narita, *Physica B+C* **139-140**, 397 (1986); K. Akiba, A. Miyake, Y. Akahama, K. Matsubayashi, Y. Uwatoko, and M. Tokunaga, *Phys. Rev. B* **95**, 115126 (2017).
 - [22] J. Guo, H. Wang, F. von Rohr, W. Yi, Y. Zhou, Z. Wang, S. Cai, S. Zhang, X. Li, Y. Li, J. Liu, K. Yang, A. Li, S. Jiang, Q. Wu, T. Xiang, R. J. Cava, and L. Sun, *Phys. Rev. B* **96**, 224513 (2017).
 - [23] T. Kikegawa and H. Iwasaki, *Acta Crystallogr., Sec. B: Struct. Sci.* **39**, 158 (1983).
 - [24] J. C. Jamieson, *Science* **139**, 1291 (1963).
 - [25] M. Imada, A. Fujimori, and Y. Tokura, *Rev. Mod. Phys.* **70**, 1039 (1998).
 - [26] G. Kotliar, S. Y. Savrasov, K. Haule, V. S. Oudovenko, O. Parcollet, and C. A. Marianetti, *Rev. Mod. Phys.* **78**, 865 (2006).
 - [27] M. F. Pereira Jr. and K. Henneberger, *Phys. Status Solidi B* **206**, 477 (1998); D. S. Chemla and J. Shah, *Nature (London)* **411**, 549 (2001); J. M. Tomczak, K. Haule, T. Miyake, A. Georges, and G. Kotliar, *Phys. Rev. B* **82**, 085104 (2010).
 - [28] P. Sun, W. Xu, J. M. Tomczak, G. Kotliar, M. Sondergaard, B. B. Iversen, and F. Steglich, *Phys. Rev. B* **88**, 245203 (2013).
 - [29] L. Craco, M. S. Laad, and E. Müller-Hartmann, *Phys. Rev. Lett.* **90**, 237203 (2003).

- [30] P. Jarillo-Herrero, J. Kong, H. S. J. van der Zant, C. Dekker, L. P. Kouwenhoven, and S. De Franceschi, *Nature (London)* **434**, 484 (2005).
- [31] J. Kondo, *Prog. Theor. Phys.* **32**, 37 (1964).
- [32] A. C. Hewson, *The Kondo Problem to Heavy Fermions* (Cambridge University Press, Cambridge, 1993).
- [33] A. Georges, G. Kotliar, W. Krauth, and M. J. Rozenberg, *Rev. Mod. Phys.* **68**, 13 (1996).
- [34] K. Sengupta and G. Baskaran, *Phys. Rev. B* **77**, 045417 (2008).
- [35] J. Jobst, F. Kisslinger, and H. B. Weber, *Phys. Rev. B* **88**, 155412 (2013).
- [36] L. Craco and S. Leoni, *Sci. Rep.* **5**, 13772 (2015).
- [37] L. Craco, M. S. Laad, S. Leoni, and A. S. de Arruda, *Phys. Rev. B* **87**, 155109 (2013).
- [38] J.-H. Chen, L. Li, W. G. Cullen, E. D. Williams, and M. S. Fuhrer, *Nat. Phys.* **7**, 535 (2011); M. Hentschel and F. Guinea, *Phys. Rev. B* **76**, 115407 (2007).
- [39] L. Fritz and M. Vojta, *Rep. Prog. Phys.* **76**, 032501 (2013).
- [40] S. Barua, M. C. Hatnean, M. R. Lees, and G. Balakrishnan, *Sci. Rep.* **7**, 10964 (2017).
- [41] See, for example, Y. Katayama and S. Tanaka, *Phys. Rev.* **153**, 873 (1967); Y. Xu, J. Zhang, G. Cao, C. Jing, and S. Cao, *Phys. Rev. B* **73**, 224410 (2006).
- [42] O. K. Andersen, *Phys. Rev. B* **12**, 3060 (1975).
- [43] V. Antonov, B. Harmon, and A. Yaresko, *Electronic Structure and Magneto-Optical Properties of Solids* (Kluwer Academic Publishers, Dordrecht, Boston, London, 2004); see also, S. Chadov, X. Qi, J. Kübler, G. H. Fecher, C. Felser, and S. C. Zhang, *Nat. Mater.* **9**, 541 (2010).
- [44] M. S. Laad, L. Craco, and E. Müller-Hartmann, *Phys. Rev. B* **73**, 045109 (2006).
- [45] L. Craco, *Phys. Rev. B* **77**, 125122 (2008).
- [46] N. Dasari, W. R. Mondal, P. Zhang, J. Moreno, M. Jarrell, and N. S. Vidhyadhiraja, *Eur. Phys. J. B* **89**, 202 (2016).
- [47] H. Kajueter and G. Kotliar, *Phys. Rev. Lett.* **77**, 131 (1996).
- [48] V. Y. Klevets, N. D. Savchenko, T. N. Shchurova, I. I. Opachko, and K. O. Popovic, *Funct. Mater.* **20**, 97 (2013).
- [49] Th. Pruschke, R. Bulla, and M. Jarrell, *Phys. Rev. B* **61**, 12799 (2000).
- [50] C. Grenzbach, F. B. Anders, G. Czycholl, and T. Pruschke, *Phys. Rev. B* **74**, 195119 (2006).
- [51] L. Craco, M. S. Laad, S. Leoni, and H. Rosner, *Phys. Rev. B* **77**, 075108 (2008).
- [52] L. Craco, J. L. B. Faria, and S. Leoni, *Mater. Res. Express* **4**, 036303 (2017).
- [53] L. Craco, M. S. Laad, and S. Leoni, *Sci. Rep.* **7**, 2632 (2017).
- [54] M. S. Laad and L. Craco, *Phys. Rev. B* **84**, 054530 (2011).
- [55] A. A. Burkov, *Nat. Mater.* **15**, 1145 (2016).
- [56] L. Craco and S. Leoni, *Phys. Rev. B* **85**, 075114 (2012); **85**, 195124 (2012).